Available online at www.sciencedirect.com
SCIENCE DIRECT®
Composite Structures 68 (2005) 53–63
COMPOSITE STRUCTURES
www.elsevier.com/locate/compstruct

The estimate of the effect of z-pins on the strain release rate, fracture and fatigue in a composite co-cured z-pinned double cantilever beam

Larry W. Byrd [a], Victor Birman [b,*]

[a] Air Force Research Laboratory, AFRL/VASM, Building 65, 2700 D Street, Wright-Patterson Air Force Base, OH 45433-7402, USA
[b] University of Missouri-Rolla, Engineering Education Center, 8001 Natural Bridge Road, St. Louis, MO 63121-4499, USA

Available online 9 April 2004

Abstract

The paper illustrates the effect of z-pins on the strain energy release rate in composite co-cured double cantilever beams (DCB) subject to a standard fracture toughness test. The conclusions obtained as a result of the solution illustrate that z-pins can provide drastic enhancement in fatigue and fracture properties of a co-cured z-pinned composite joint, even if their volume fraction is low. The strain energy release rate for loading and geometry combinations that do not result in immediate fracture was significantly reduced as a result of using z-pins. This slows the rate of the crack propagation if it is governed by the Paris law. Moreover, z-pins can completely arrest the crack. Although the analysis was performed for DCB specimens, the conclusions can be extrapolated to a general case of co-cured z-pinned joints.

Keywords: Double-cantilever beam; Z-pinned joint; Fracture; Fatigue; Crack

1. Introduction

Delamination cracks originating from the edge of the joint are recognized as the principal cause of damage and failure in bonded adhesive and co-cured joints. Z-pins represent a possible method of arresting or slowing these cracks. In particular, this method may be effective in enhancing fracture and fatigue resistance of co-cured joints between composite skin and stiffeners depicted in Fig. 1. However, a detailed analysis of the effect of z-pins on fracture toughness of such joints has not been published.

Early studies of the effect of z-pins on the integrity of laminated structures have been published by Freitas et al. [1], Lin and Chan [2], Palazotto et al. [3] and others. The recent work by Rugg et al. [4] was concerned with the effectiveness of z-pins in a skin-stiffener joint. One of the conclusions from this work was that z-pins can completely suppress delaminations originating from the edge of the flange. In the present paper the effectiveness of z-pins is estimated on the example of a standard DCB test prescribed for composite adhesive joints (though an adhesive layer is not used in co-cured joints). A typical setup of the test is presented in Fig. 2 [5].

Examples of early studies that attempted to evaluate the stress intensity factor or fracture toughness of DCB are the papers of Ripling et al. [6], Gross and Srawley [7], Srawley and Gross [8] and Fichter [9]. These papers did not account for all factors that affect the fracture problem of DCB, including the finite resistance of the beam to rotations at the tip of the crack. This rotational resistance was taken into account in the work of Kanninen [10] and in other references referred to below.

The present solution employs the analysis of DCB that is based on modeling the effect of a limited rotational constraint of the intact part of the beam (see Fig. 3, $x > 0$) through the introduction of an elastic foundation. Such approach was originally proposed by Kanninen [10,11]. It was further extended to transversely isotropic materials by Williams [12] and to angle-ply laminates by Ozdil and Carlsson [13]. Penado [14] used the same approach to incorporate the effect of an adhesive layer between the two halves of the beam. In the present paper, the method developed in the references

* Corresponding author. Tel.: +1-314-516-5431; fax: +1-314-516-5434.
E-mail address: vbirman@umr.edu (V. Birman).

0263-8223/$ - see front matter © 2004 Elsevier Ltd. All rights reserved.
doi:10.1016/j.compstruct.2004.02.014

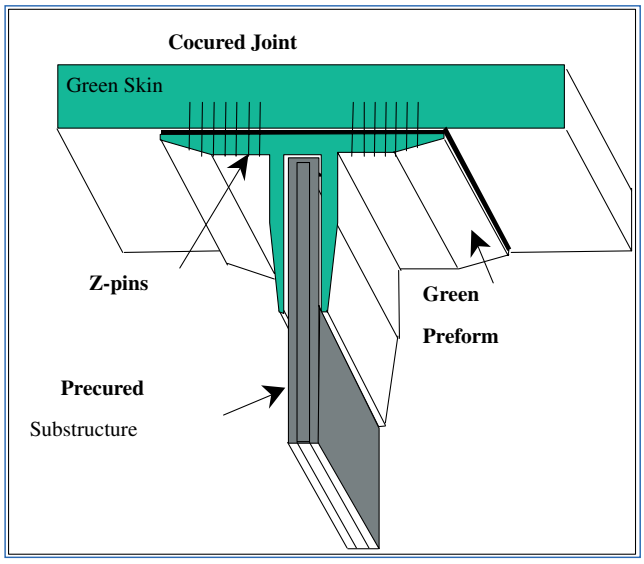

Fig. 1. Co-cured z-pinned joint between the skin and stiffener.

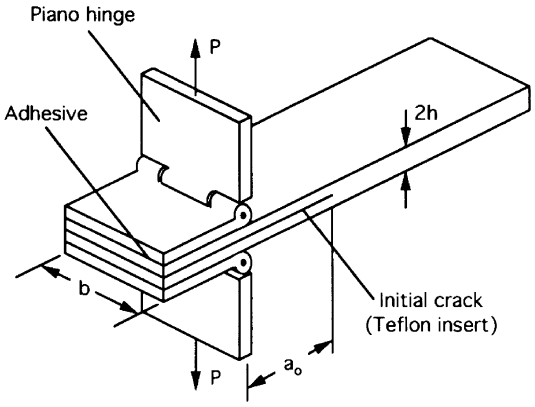

Fig. 2. Schematic illustration of the DCB test, according to ASTM 5528 [5].

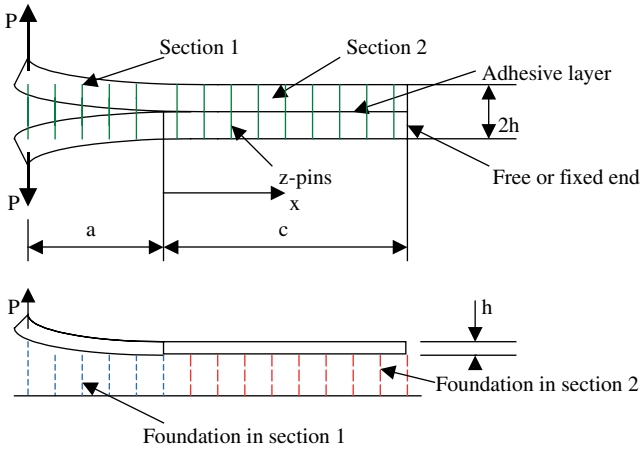

Fig. 3. DCB with z-pins loaded in mode I and the model used in the analysis. The stiffnesses of foundation in Sections 1 and 2 are different.

listed above is extended through modeling the effect of z-pins as an elastic foundation in both delaminated and intact sections of DCB (Fig. 3).

It is useful to note that the solution for Mode I fracture toughness of elastic DCB specimens shown in Fig. 2 is given by

$$G_{IC} = \frac{P_c^2}{2b}\frac{dC}{da} \tag{1}$$

where P_c is the fracture load, b is the width of the specimen and $\frac{dC}{da}$ is the rate of change of the compliance per unit crack growth.

2. Analysis

Consider the response of Sections 1 and 2 of the beam shown in Fig. 3. The present solution is limited to the case where the length of the crack remains small, i.e. $a \ll c$. Accordingly, the separation between the delaminated parts of the beam in Section 1 is sufficiently small to assume that the pins in this section remain partially embedded within the joint material (i.e. there is no pullout of z-pins from Section 1). The nonlinear force-pullout displacement response of the pins includes the initial linear relationship corresponding to the situation where the motion of the pin relative to the matrix material is limited to the zone adjacent to the crack plane [15]. After the entire interface between the pin and matrix is affected, the force applied by the pin to the matrix decreases yielding the following pressure on the delaminated section [16]:

$$p = K_0 - K_1 w \quad K_0 = 2V_p \tau l_p / r \quad K_1 = 4V_p \tau / r \tag{2}$$

where V_p denotes the areal density of pins, l_p and r are the pin embedded length (usually it is equal to the thickness of the delaminated section h) and radius, respectively, and τ is the interfacial shear strength. The initial linear force-pullout displacement part of the response can often be neglected since it corresponds to very small deflections, in which case (2) represents the reaction of the pins in Section 1.

In Section 2, the pins do not experience pullout action. However, jointly with the second (bottom) half-thickness of DCB, they restrict rotations of the delaminated section. The stiffness of the equivalent elastic foundation provided by the z-pins and by the lower half-thickness of the intact beam is obtained as

$$k_2 = k_p + k_b \tag{3}$$

where $k_p = \frac{nV_pE_p}{h}$, $k_b = \frac{n(1-V_p)E_z}{h}$. In these equations, E_p and E_z are the moduli of the pin and composite material in the thickness direction, respectively. The factor n can be chosen rather subjectively. For example, this factor was taken equal to $n = 2$ in the papers of Kanninen [10] and Ozdil and Carlsson [13]. This value is obtained if the

average transverse strain is defined as a ratio of the total relative displacement of the upper and lower halves of the beam ($2w_2$) to the distance between the centroids of these halves (h). Numerical results obtained using such factor were in good agreement with the experimental data. Penado [14] used $n = 4$ (this choice seems to be less logical). However, his results were in good agreement both with FEA and with the results generated using $n = 2$ for all materials and geometries considered in his paper. The exception was the case of a very short crack ($h/a \geqslant 0.5$). In this case (not considered here), the solution of Penado was more accurate. Note that all these papers, i.e. [10,13,14], were concerned with adhesive joints without z-pins.

In the present work, the following approach is employed to evaluate the magnitude of the factor n. Consider each of two halves of the beam shown in Fig. 3 as a thin beam. In this case, deflections w remain constant through the thickness of each half-beam at a given cross-section $x = \text{const}$. Therefore, the average transverse strain through the thickness of the intact part of the beam can be estimated as $\varepsilon_z = \frac{2w_2}{2h} = \frac{w_2}{h}$. Using this strain in equations

$$\begin{aligned} \sigma_z &= [V_p E_p + (1 - V_p)E_z]\varepsilon_z \\ k_2 &= \frac{\sigma_z}{w_2} \end{aligned} \tag{4}$$

yields $n = 1$. The comparison between the results obtained for the values of $n = 1$, 2, 4 is presented in numerical examples.

Note that the effective bending modulus is needed for the solution shown below. This modulus can be determined either by the procedure recommended by Ozdil and Carlsson [13] or by the method recommended in the monograph of Gibson [17]. The presence of z-pins changes the effective modulus in the x-direction since the laminate and z-pins work in parallel. Accordingly, for the jth layer,

$$\frac{1}{(E_x)_j} = \frac{1 - V_p}{E_{1j}} + \frac{V_p}{E_p} \tag{5}$$

where E_{1j} is the modulus of the layer in the axial direction.

In the following analysis, each section of the beam is considered as a thin beam, i.e. transverse shear and peeling stresses are neglected. Obviously, such assumption can be questionable if the ratio a/h is small. However, as was shown by Penado [14], the error due to neglecting the effect of transverse shear stresses becomes noticeable only if $a/h < 10$. Even if this ratio is in the range between 5 and 10, the error was in an acceptable range (less than 5% for unidirectional E-glass/epoxy and aluminum and less than 16% for unidirectional graphite/epoxy). In the following examples, the ratio a/h was higher than 9.1, except for the case considered in Fig. 9 where this ratio was higher than 4.6 and Figs. 11 and 13 where this ratio was higher than 6.8 and 5.7, respectively. Obviously, a more accurate analysis accounting for three-dimensional stresses is needed in case of short cracks. Such analysis will be conducted in the future study.

The response of Section 2 of the beam is governed by the standard bending equation of the beam on the linear elastic foundation. The solution obtained by assumption that the length of the section is much larger than that of the crack (semi-infinite beam) implies that displacements should remain limited at $x \to \infty$. Accordingly,

$$w_2 = e^{-\lambda_2 x}(A_2 \sin \lambda_2 x + B_2 \cos \lambda_2 x) \tag{6}$$

where $\lambda_2 = \sqrt[4]{\frac{3k_2}{E_x h^3}}$ and E_x is the bending modulus of the material.

Note that the assumption that the boundary conditions at the right end of the beam do not affect the solution is justified in most situations. For example, Kanninen [10] showed that the effect of the right end is negligible if the length of Section 2 exceeds $2h$.

The response of Section 1 is obtained by solving the equilibrium equation

$$\frac{d^4 w_1}{dx^4} + \frac{12}{E_x h^3}(-K_1 w_1 + K_0) = 0 \tag{7}$$

The solution is

$$\begin{aligned} w_1 = {} & A_1 \cos \lambda_1 x + B_1 \sin \lambda_1 x + C_1 \cosh \lambda_1 x \\ & + D_1 \sinh \lambda_1 x + \frac{K_0}{K_1} \end{aligned} \tag{8}$$

where $\lambda_1 = \sqrt[4]{\frac{12K_1}{E_x h^3}}$. The effect of a partial z-pin pullout on the bending modulus of Section 1 was found sufficiently small to be neglected in this solution.

The deflection of the loaded end of Section 1 can now be determined and subsequently, the compliance of the DCB specimen can be obtained as $C = \frac{2w_1(-a)}{P}$, according to the ASTM standard (ASTM, D 5528). The rate of change of this compliance as a function of the crack length that is necessary to evaluate fracture toughness by (1) can be derived analytically or, more conveniently, obtained from the compliance-crack length curve $C(a)$.

The following boundary and continuity conditions can be employed to specify the constants of integration in (6) and (8):

$$\begin{aligned} & w_1(0) = w_2(0) \quad w_1'(0) = w_2'(0) \\ & w_1''(0) = w_2''(0) \quad w_1'''(0) = w_2'''(0) \\ & w_1''(-a) = 0 \quad w_1'''(-a) = \frac{12P}{E_x b h^3} \end{aligned} \tag{9}$$

The substitution of (6) and (8) into (9) yields a set of algebraic equations for the constants of integration:

$$\begin{bmatrix} a_{11} & a_{12} & a_{13} & a_{14} & a_{15} & a_{16} \\ a_{21} & a_{22} & a_{23} & a_{24} & a_{25} & a_{26} \\ a_{31} & a_{32} & a_{33} & a_{34} & a_{35} & a_{36} \\ a_{41} & a_{42} & a_{43} & a_{44} & a_{45} & a_{46} \\ a_{51} & a_{52} & a_{53} & a_{54} & a_{55} & a_{56} \\ a_{61} & a_{62} & a_{63} & a_{64} & a_{65} & a_{66} \end{bmatrix} \begin{Bmatrix} A_1 \\ B_1 \\ C_1 \\ D_1 \\ A_2 \\ B_2 \end{Bmatrix} = \begin{Bmatrix} b_1 \\ b_2 \\ b_3 \\ b_4 \\ b_5 \\ b_6 \end{Bmatrix} \tag{10}$$

where

$$a_{11} = a_{13} = 1 \quad a_{12} = a_{14} = a_{15} = 0 \quad a_{16} = -1$$

$$b_1 = -\frac{K_0}{K_1}$$

$$a_{21} = a_{23} = b_2 = 0 \quad a_{22} = a_{24} = \lambda \quad a_{25} = -1 \quad a_{26} = 1$$

$$a_{31} = -a_{33} = \frac{\lambda^2}{2} \quad a_{32} = a_{34} = a_{36} = b_3 = 0 \quad a_{35} = -1$$

$$a_{41} = a_{43} = b_4 = 0 \quad a_{42} = -a_{44} = \frac{\lambda^3}{2} \quad a_{45} = a_{46} = 1$$

$$a_{51} = -\cos(\lambda_1 a) \quad a_{52} = \sin(\lambda_1 a) \quad a_{53} = \cosh(\lambda_1 a)$$

$$a_{54} = -\sinh(\lambda_1 a) \quad a_{55} = a_{56} = b_5 = 0$$

$$a_{61} = -\sin(\lambda_1 a) \quad a_{62} = -\cos(\lambda_1 a) \quad a_{63} = -\sinh(\lambda_1 a)$$

$$a_{64} = \cosh(\lambda_1 a) \quad a_{65} = a_{66} = 0 \quad b_6 = \frac{12P}{E_x b h^3 \lambda_1^3}$$

$$\lambda = \frac{\lambda_1}{\lambda_2} \tag{11}$$

Once the constants of integration are calculated, the deflection of the loaded end of the cantilever can be determined:

$$w_1(-a) = \frac{K_0}{K_1} + A_1 \cos(\lambda_1 a) - B_1 \sin(\lambda_1 a) + C_1 \cosh(\lambda_1 a) - D_1 \sinh(\lambda_1 a) \tag{12}$$

3. Numerical examples

The investigation of the effectiveness of z-pins in co-cured composite joints was carried out for three different material systems that are outlined in Table 1.

The first material in Table 1 is E-glass/epoxy used by Ozdil and Carlsson [13] in their analysis of laminated DCB (this study did not consider the effect of z-pins). Carbon/epoxy (AS4/3501-6) was employed by Rugg et al. [4] in their investigation of the effect of z-fibers on delamination resistance of composite mixed-mode bending laminates. Finally, CMC (SiC/CAS) in Table 1 was considered by Domergue et al. in their research [18,19]. In all examples shown below, E-glass/epoxy and SiC/CAS specimens were assumed unidirectional, with the fibers oriented in the x-direction.

The thickness of each delaminated "leg" of DCB was taken equal to $h = 2.19$ mm, following the work of Ozdil and Carlsson [13]. The width of the specimens was $b = 20$ mm. The radius of titanium z-pins was equal to 0.47 mm as in the paper of Rugg et al. [4]. The radius of carbon pins was equal to either 0.6 mm (SiC/CAS beams) or 0.47 mm (E-glass/epoxy beams).

The interfacial shear strength between z-pins and composite material is usually unknown. Therefore, this strength was assumed equal to 20 MPa, in all cases. Note that this value is also close the fiber push-out sliding resistance for SiC/CAS material [18]. The factor $n = 1$ was used in all examples, except for Fig. 15.

The effect of z-pin volume fraction on the deflection of the delaminated (free) end of DCB and on its compliance is shown for E-glass/epoxy (Fig. 4), carbon/epoxy (Figs. 5–7) and SiC/CAS (Fig. 8). In all cases, the length of the crack was equal to $a = 20$ mm. The choice of the applied force was dictated by the limitations on the deflection of the delaminated end. If $w_1(-a) > h$, the pins at the free end are pulled out of the composite material. In this case, the problem becomes more complicated since it is necessary to analyze three sections of the beam. These include Section 2, and Section 1 that should be subdivided into the subsection where the pins have been pulled out and a subsection, adjacent to Section 2 where the pins are still embedded into the material. The results shown below indicate that the rate of the change in the compliance abruptly increases as the deflections approach the pullout value. Therefore, it may be reasonable to assume that the specimen fails as $w_1(-a) \to h$. The other consideration limiting the applied load is the strength of the delaminated section of the beam. This problem is also discussed below. While the upper limit of the applied load is governed by the reasons outlined in this paragraph, if the load is too small, it cannot overcome the resistance provided by the pins (this is due to the term K_0 in the expression for the equivalent elastic foundation).

As follows from Figs. 4–8, an increase in the volume fraction of z-pins results in a reduction of the deflections of the free end of DCB. This is obviously due to the effect of the elastic foundation provided by z-pins.

Table 1
Materials used in the analysis of co-cured z-pinned composite joints

Composite material	E_1 (GPa)	E_z (GPa)	Z-pin material	E_p (GPa)
E-glass/epoxy	34.7	8.5	Carbon, $r = 0.47$ mm	190.0
Plain-woven AS4/3501-6 (carbon/epoxy)	57.2	9.53	titanium	115.0
SiC/CAS	140.0	130.0	Carbon, $r = 0.6$ mm	190.0

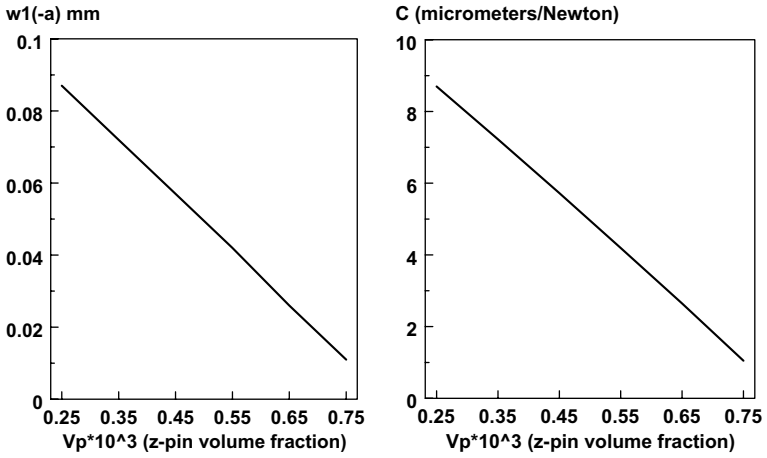

Fig. 4. Effect of z-pin volume fraction on the free-end deflection and compliance of E-glass/epoxy DCB. The length of the crack is $a = 20$ mm, the applied force is $P = 20$ N.

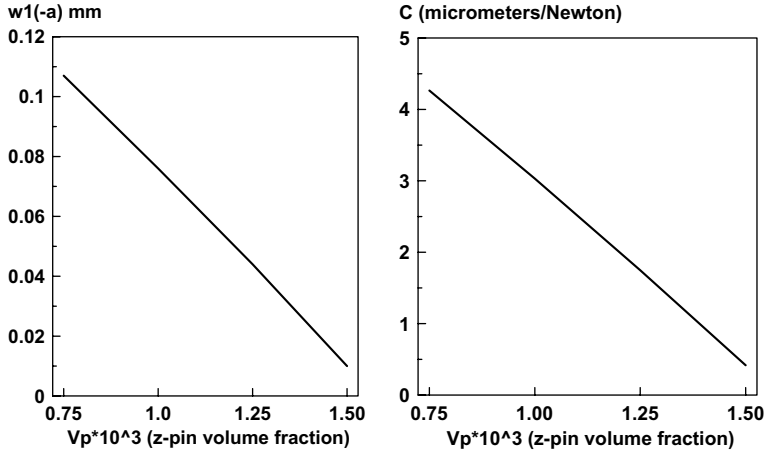

Fig. 5. Effect of z-pin volume fraction on the free-end deflection and compliance of plain-woven AS4/3501-6 carbon/epoxy DCB. The length of the crack is $a = 20$ mm, the applied force is $P = 50$ N.

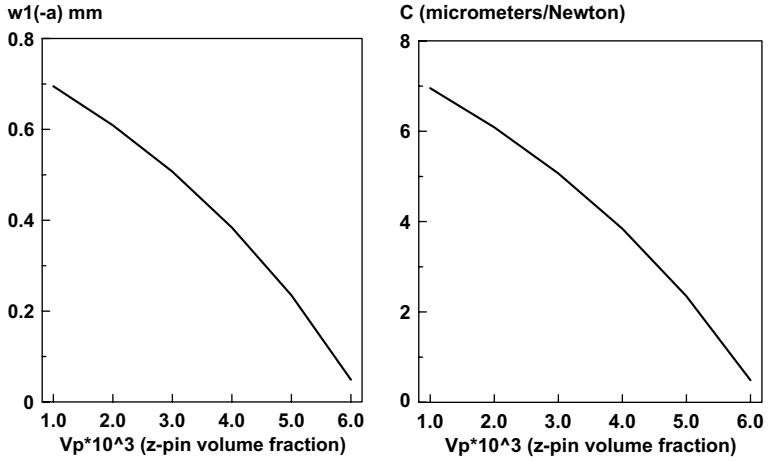

Fig. 6. Effect of z-pin volume fraction on the free-end deflection and compliance of plain-woven AS4/3501-6 carbon/epoxy DCB. The length of the crack is $a = 20$ mm, the applied force is $P = 200$ N.

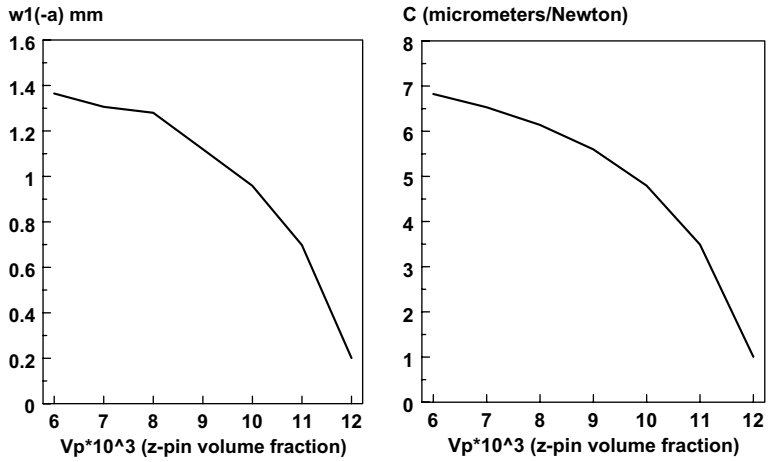

Fig. 7. Effect of z-pin volume fraction on the free-end deflection and compliance of plain-woven AS4/3501-6 carbon/epoxy DCB. The length of the crack is $a = 20$ mm, the applied force is $P = 400$ N.

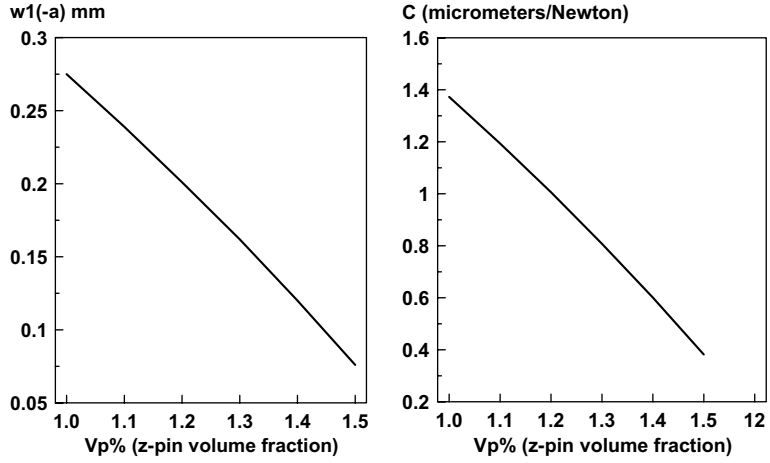

Fig. 8. Effect of z-pin volume fraction on the free-end deflection and compliance of SiC/CAS DCB. The length of the crack is $a = 20$ mm, the applied force is $P = 400$ N.

Interestingly, at a certain volume fraction of z-pins, the deflections of the free end become equal to zero and the subsequent increase in the z-pin volume fraction actually produces negative deflections. This phenomenon is due to exceedingly high total stiffness of the foundation. Naturally, negative deflections are physically impossible. Instead, zero deflections should be identified with a complete arrest of the crack. Such phenomenon was reported for z-pinned laminates by Rugg et al. [4] who noticed a change from delamination mode of failure to microbuckling, as a result of the introduction of z-pins. Notably, even a very small volume fraction of z-pins is sufficient to either drastically reduce deflections or completely arrest the crack. This volume fraction becomes particularly small, if the difference between the modulus of elasticity of the composite material and that of the pins increases. For example, deflections were almost eliminated in an E-glass/epoxy DCB with a 20-mm crack by introducing z-pins with the volume fraction equal to just 0.075% (Fig. 4).

The compliance was also reduced as a result of a higher z-pin volume fraction reflecting on a positive effect of z-pins. Both the deflections as well as the compliance increased with a larger applied force, as follows from the comparison of Figs. 5–7 (and from Fig. 12 discussed below).

It is necessary to emphasize that the applicability of the present solution should be analyzed keeping in mind a possible loss of strength of the cantilever section of DCB. A quick estimate of the strength can be conducted by analyzing this section as a cantilever subject to the end lateral force. The maximum stress in the cantilever with the clamped end is

$$\sigma_{\max} = \frac{6Pa}{bh^2} \tag{13}$$

This stress should be compared to the strength of DCB in the x-direction. Apparently, neither glass/epoxy nor carbon/epoxy DCB fail under the conditions considered in Figs. 4–7.

The situation is different in the case of a SiC/CAS specimen. This is related to the emergence of bridging matrix cracks perpendicular to the fibers. In case of bending of a delaminated cantilevered leg of DCB, these cracks will first form in the layers on the tensile surface of the leg (Section 1), at $x = 0$. The matrix cracking stress for the material considered in the examples is close to 285 MPa. It is easy to predict that the onset of the cracks in the fully clamped section will occur at the force $P = 356$ N. However, in reality, the applied force corresponding to matrix cracking should be higher since the "clamped end" of Section 1 is actually elastically constrained against rotations, i.e. the results shown in Fig. 8 are still reliable.

The effect of the length of the crack on the free-end deflections and DCB compliance are illustrated in Fig. 9 for carbon/epoxy DCB and in Figs. 10 and 11 for SiC/CAS DCB. Note that while the length of the cracks considered in Figs. 10 and 11 may justify the analysis based on the technical theory of beams, the cracks considered for carbon/epoxy are quite short. This implies that numerical values in Fig. 9 should be treated with caution, although the quantitative conclusions are valid since they confirm the results shown in Figs. 10 and 11. The reason longer cracks are not considered in Figs. 9–11 is related to excessive deflections of the free end in case of long cracks and the resulting pullout of z-pins that is not accounted for in the present solution. As

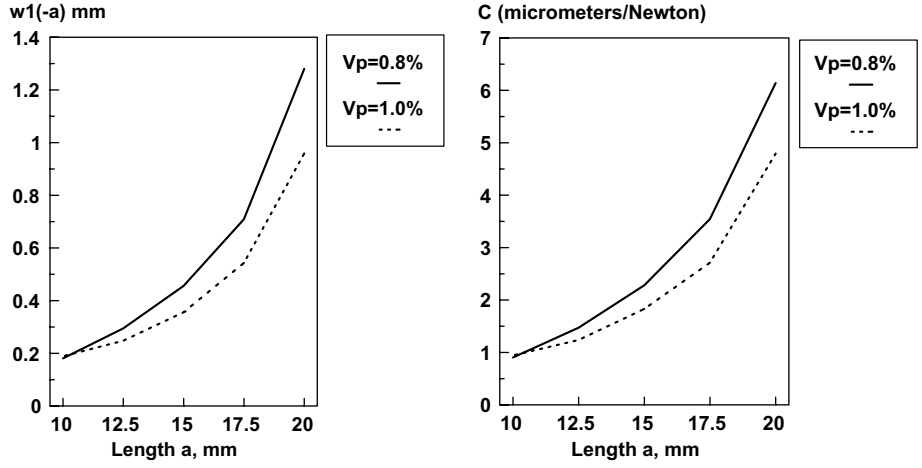

Fig. 9. Effect of the length of the crack on the free-end deflection and compliance of plain-woven AS4/3501-6 carbon/epoxy DCB. The applied force is $P = 400$ N.

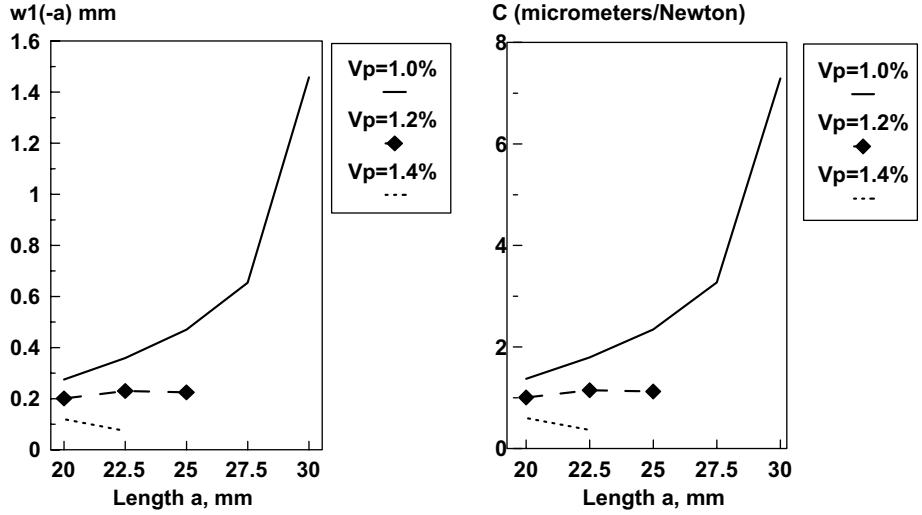

Fig. 10. Effect of the length of the crack on the free-end deflection and compliance of SiC/CAS DCB. The applied force is $P = 400$ N.

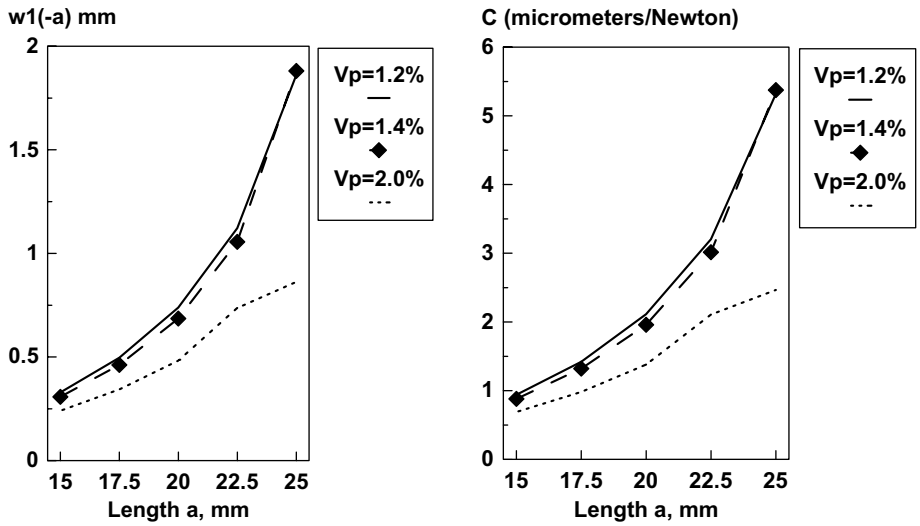

Fig. 11. Effect of the length of the crack on the free-end deflection and compliance of SiC/CAS DCB. The applied force is $P = 700$ N.

follows from the results shown in these figures, deflections of the free end are predictably smaller, if the crack is short.

It is interesting to note that if the applied force is not sufficiently large, the deflections of the free end may actually decrease, as the crack becomes longer (Fig. 10). This is related to a large cumulative effect of z-pins that can "overcome" the effect of the applied force, particularly if their volume fraction is high. Even if the force is equal to 700 N (Fig. 11), the effect of z-pins seems to become dominant for longer cracks (see the case of $V_p = 2\%$).

Note that the results shown in Fig. 11 do not account for a reduction in the elastic modulus due to matrix cracking on the tensile surface of the cantilevered section of DCB. However, the strength of the section is not compromised, even if the matrix cracks appear, since the tensile strength of Nicalon fibers is close to 2.75 GPa [20]. Considering the fact that the fiber volume fraction is about 40%, this should guarantee sufficient strength of the specimens considered in Fig. 11.

In general, as the cracks become longer, one of two tendencies dominates. The deflections may become so large that z-pins will be pulled out of Section 1. In this case, the rate of change in the compliance abruptly increases implying an almost immediate failure. On the other hand, if the force is not sufficiently large, the crack can be arrested (in the present analysis, this is associated with a reduction of the deflections that approach zero).

The effect of the applied force on the deflections and compliance is illustrated in Fig. 12 for a SiC/CAS specimen. The results may be affected by matrix cracking on the tensile surface, but the general tendencies are obvious. Deflections increase almost proportionally to the magnitude of the applied force (if the length of the crack is constant). The compliance also increases with larger forces. Although the rate of this increase in compliance is reduced at large values of the applied force, it is anticipated that matrix cracking should avert this tendency.

The change in the rate of the compliance is shown as a function of the crack length in Figs. 13 (carbon/epoxy) and 14 (SiC/CAS). The conclusion from Fig. 13 is that a higher z-pin volume fraction results in a smaller rate of the change in the compliance for the most part of the fatigue life. On the other hand, in the immediate vicinity of the crack length corresponding to the onset of pin pullout, the rate of the change in compliance is much higher if the pin density increases. In general, both Figs. 13 and 14 illustrate an abrupt increase of $\mathrm{d}C/\mathrm{d}a$ at the "critical" length of the crack corresponding to a dramatic increase in deflections $w_1(-a)$, pullout of z-pins, and, probably, immediate fracture.

The results discussed in the last paragraph have important implications on the fatigue life of the specimen. For example, the rate of fatigue crack propagation is often governed by the Paris-type equation

$$\frac{\mathrm{d}a}{\mathrm{d}N} = k(\Delta G)^m \tag{14}$$

where N is the number of cycles, k, m are material constants, and ΔG is the range of the strain energy release rate during the cycle. The introduction of z-pins clearly reduces ΔG for the entire fatigue life, except for the final phase preceding fracture. If one assumes that constants k, m are little affected by the presence of z-pins, it is obvious that the rate of crack propagation should be reduced in z-pinned joints.

It is also important to estimate an effect of z-pins on the critical failure load P_c. The following approach can address this issue.

In experiments on plain-woven AS4/3501-6 mixed-mode joints, Rugg et al. [4] presented results for the

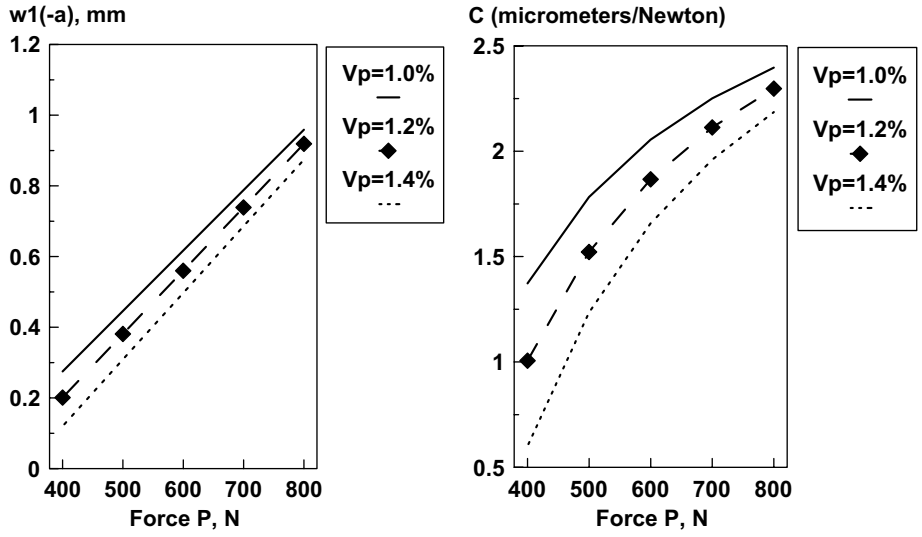

Fig. 12. Effect of the applied force on the free-end deflection and compliance of SiC/CAS DCB. The length of the crack is $a = 20$ mm.

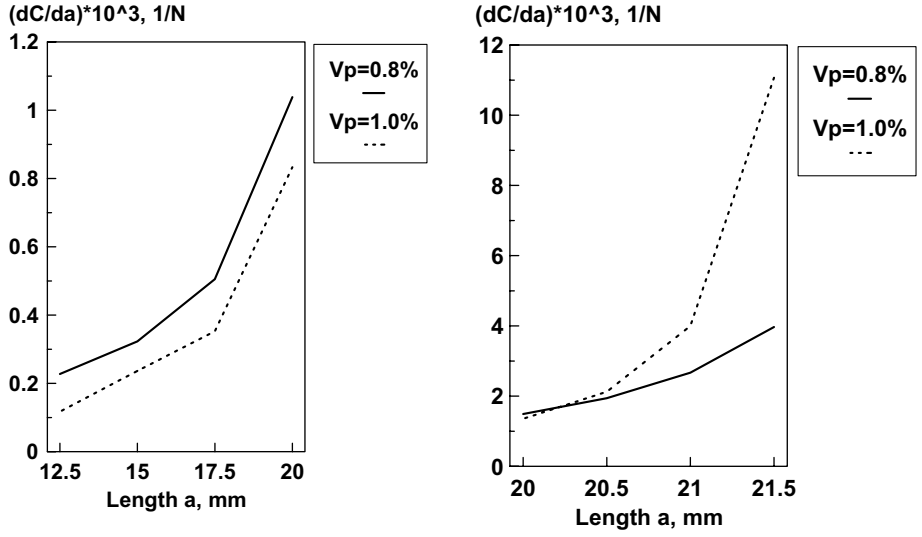

Fig. 13. Effect of the length of the crack on the rate of change in compliance of plain-woven AS4/3501-6 carbon/epoxy DCB. The applied force is $P = 400$ N.

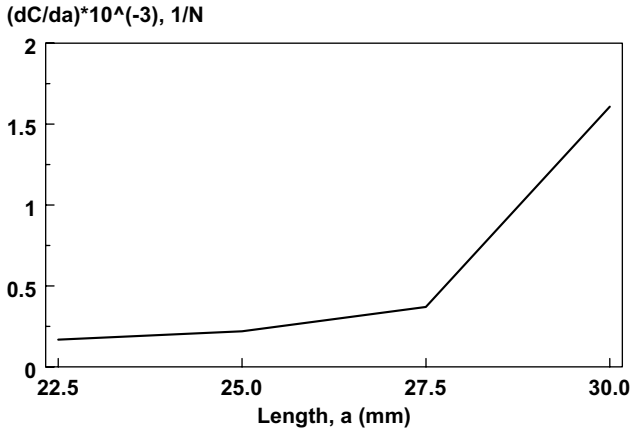

Fig. 14. Effect of the length of the crack on the rate of change in compliance of SiC/CAS DCB. The applied force is $P = 400$ N.

applied load corresponding to failure as a function of the volume fraction of z-pins (see [4, Figs. 3 and 4]). Although the present work is concerned with Mode I fracture, the results in [4]. are still instructive for an estimate of the effect of z-pins on the failure load.

It is assumed here that the failure load is proportional to the strength of the specimen in the thickness (z) direction. This strength is obtained by the rule of mixtures:

$$s_z = V_p s_p + (1 - V_p) s_c \tag{15}$$

where s_p and s_c are tensile strengths of the pin and composite materials, respectively.

Tensile transverse strength of AS4/3501-6 is 48.0 MPa, while Ti–6Al-4V pins used in the work of Rugg et al. [4] have the yield strength equal to 1100 MPa and

the ultimate strength of 1235 MPa. The results presented in [4, Fig. 3] are compared to the predictions calculated according to the assumption introduced in the present report in Table 2.

In Table 2, the ratio $\frac{P_c(V_p)}{P_c(V_p=0)}$ is obtained from [4], and strength ratios (1) and (2) are obtained using the yield strength and the ultimate strength of the pins, respectively. As follows from Table 2, the change in the strength of the joint in the thickness direction calculated using the ultimate strength of z-pins can serve as a reliable indicator of the change in the failure load.

The same conclusion follows from the analysis of Fig. 4 of Rugg et al. [4]. In the case where the volume fraction of z-pins is equal to 2%, the experimental increase in the failure load and the increase calculated using the ultimate strength of z-pins were equal to the factors 1.47 and 1.49, respectively. It was impossible to compare the prediction to the results for $V_p = 4\%$ in the same figure since the mode of failure was skin buckling, rather than delamination cracking.

Finally, the effect of the factor n in the expression for the stiffness of elastic foundation of the intact section (Section 2) on the accuracy of results is analyzed in Fig. 15. As indicated above, the calculations were performed with $n = 1$, while other sources referenced above used the values of 2 and 4. Accordingly, a difference between the deflection of the free end and compliance of a SiC/CAS DCB is considered for these values of n. As follows from Fig. 15, the effect of the factor n on deflections and compliance is quite small, except for the length of the crack that approaches the critical value. However, even for $a = 30$ mm, the difference between deflections of the free end (as well as compliance) obtained using $n = 1$ and $n = 2$ was equal to 15.8%. The corresponding number for deflections and compliance calculated for $n = 1$ and $n = 4$ was 24.7%. The difference was much smaller for shorter cracks (it became almost invisible when the length of the crack was less than 25 mm).

Table 2
The increase in the failure load of carbon/epoxy joints due to the presence of z-pins

V_p	P_c (Newtons)	$\frac{P_c(V_p)}{P_c(V_p=0)}$	Strength ratio (1)	Strength ratio (2)
0	450			
1.5	641	1.42	1.33	1.37
5	1000	2.22	2.09	2.23

4. Conclusions

The paper illustrates the evaluation of the strain energy release rate for co-cured z-pinned double-cantilever beams. The general conclusions from the analysis are applicable to typical co-cured z-pinned joints.

As follows from the analysis, the rate of the change in the compliance of the delaminated DCB abruptly increases when the deflections of the free end approach the value corresponding to the pullout of z-pins from the beam. This is accompanied by an increase in the strain energy release rate that approaches the fracture toughness. If the applied load is small, the presence of z-pins can completely arrest the preexisting crack in DCB. This effect can often be reached even with a very small volume fraction of z-pins. An attempt to "force" the propagation of the crack by increasing the applied force can result in the loss of strength of the specimen, prior to achieving the conditions necessary for the propagation of the crack.

The analysis presented in the paper is limited to relatively short cracks. If the cracks are longer, the effect of

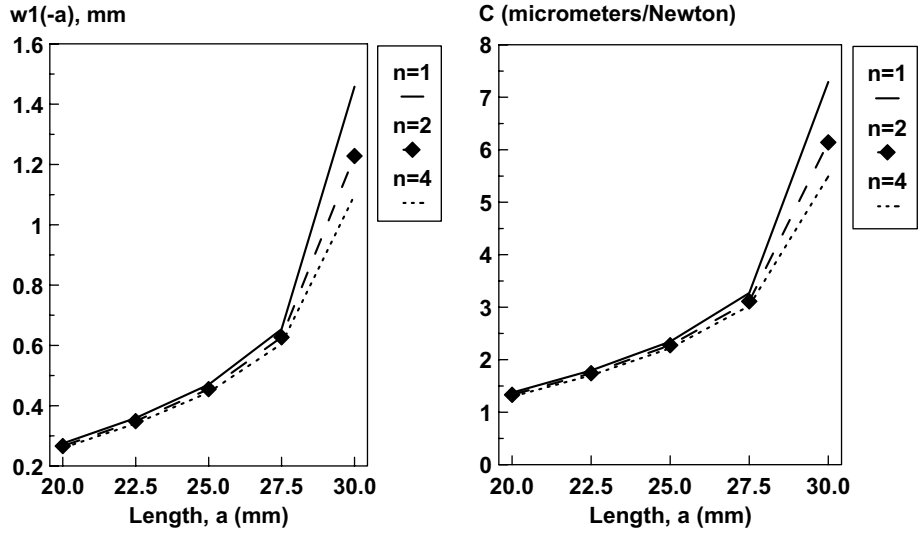

Fig. 15. Effect of the factor n in the expression for the stiffness of elastic foundation of the intact Section 2 of DCB on the accuracy of results (deflection of the free end and compliance). The applied force is $P = 400$ N, the volume fraction of z-pins is $V_p = 1\%$.

z-pins can result in their arrest. Alternatively, in the case of longer cracks, if they are not arrested, z-pins are pulled out from the region adjacent to the free delaminated end of DCB. This is usually followed with failure.

The rate of the change in the compliance (and the strain energy release rate) decreases if the volume fraction of z-pins is small, for the most part of life of DCB. However, in the vicinity of the delamination crack length corresponding to the onset of z-pin pullout and failure, a higher rate of change in the compliance corresponds to a larger z-pin volume fraction.

Based on the results presented above and their discussion, it is anticipated that the presence of z-pins would be beneficial for the fatigue life of DCB. The failure load of DCB is approximately proportional to the change in the strength in the thickness direction (direction perpendicular to the plane of the crack).

Future studies should include the effect of transverse shear deformations in the short (delaminated) section of DCB to accurately analyze short cracks. The behavior of the specimen when z-pins are completely pulled out of the part of the delaminated section represents interest since this behavior precedes failure. In addition, an analysis should be performed discarding the elastic foundation model and solving the problem using a higher order theory or a 3-D theory of elasticity. Considering the fact that either failure or a complete crack arrest occurred in the presence of z-pins when the crack was short, DCB with z-pins can be treated as a semi-infinite beam, neglecting the boundary conditions at the intact end.

Acknowledgements

This research was supported by the Air Force Office for Scientific Research Contract F33615-98-D-3210.

References

[1] Freitas G, Magee C, Dardzinski P, Fusco T. Fiber insertion process for improved damage tolerance in aircraft laminates. J Adv Mater 1994;25:36–43.

[2] Lin CY, Chan WS. Stiffness of composite laminates with Z-fiber reinforcement. AIAA Paper AIAA-99-1294, 1999.

[3] Palazotto AN, Gummadi LNB, Vaidya UK, Herup EJ. Low velocity impact damage characteristics of Z-fiber reinforced sandwich panels—an experimental study. Compos Struct 1999; 43:275–88.

[4] Rugg KL, Cox BN, Massabo R. Mixed mode delamination of polymer composite laminates reinforced through the thickness by Z-fibers. Composites Part A 2002;33:177–90.

[5] Daniel IM, Ishai O. Engineering mechanics of composite materials. New York: Oxford University Press; 1994.

[6] Ripling EJ, Mostovoy S, Patrick RL. Measuring fracture toughness of adhesive joints. Mater Res Stand 1964;4:129–34.

[7] Gross B, Srawley JE. Stress-intensity factors by boundary collocation for single-edge-notch specimens subject to splitting forces. NASA TN D-3295, 1966.

[8] Srawley JE, Gross B. Stress intensity factors for crackline-loaded edge-crack specimens. Mater Res Stand 1967;7:155–62.

[9] Fichter WB. The stress intensity factor for the double cantilever beam. Int J Fract 1983;22:133–43.

[10] Kanninen MF. An augmented double cantilever beam model for studying crack propagation and arrest. Int J Fract 1973;9:83–92.

[11] Kanninen MF. A dynamic analysis of unstable crack propagation and arrest in the DCB test specimen. Int J Fract 1974;10:415–30.

[12] Williams JG. End correction for orthotropic DCB specimens. Compos Sci Technol 1989;35:367–76.

[13] Ozdil F, Carlsson L. Beam analysis of angle-ply laminate DCB specimens. Compos Sci Technol 1999;59:305–15.

[14] Penado FE. A closed form solution for the energy release rate of the double cantilever beam specimen with an adhesive layer. J Compos Mater 1993;27:383–407.

[15] Li VC. Postcrack scaling relations for fiber reinforced cementitious composites. J Mater Civil Eng 1992;4:41–57.

[16] Mabson GE, Deobald LR. Design curves for 3D reinforced composite laminated double cantilever beams. In: Rajapakse YDS, Kardomateas GA, Birman V, editors. Mechanics of Sandwich Structures, AD-vol. 62/AMD-vol. 245. New York: American Society of Mechanical Engineers; 2000. p. 89–99.

[17] Gibson RF. Principles of Composite Material Mechanics. New York: McGraw-Hill; 1994.

[18] Domergue J-M, Vagaggini E, Evans AG. Relationships between hysteresis measurements and the constituent properties of ceramic matrix composites: II, experimental studies on unidirectional materials. J Am Ceram Soc 1995;78:2721–31.

[19] Domergue J-M, Heredia FE, Evans AG. Hysteresis loops and the inelastic deformation of 0/90 ceramic matrix composites. J Am Ceram Soc 1995;79:161–70.

[20] Schwartz MM. Composite materials, volume I: properties, nondestructive testing, and repair. Upper Saddle River, New Jersey: Prentice Hall; 1996.